International Journal of Medical Microbiology 311 (2021) 151504

Contents lists available at ScienceDirect

International Journal of Medical Microbiology

journal homepage: www.elsevier.com/locate/ijmm

Metabolic adaption of *Legionella pneumophila* during intracellular growth in *Acanthamoeba castellanii*

Mareike Kunze [a,1], Thomas Steiner [b,1], Fan Chen [b], Claudia Huber [b], Kerstin Rydzewski [a], Maren Stämmler [c], Klaus Heuner [a,*], Wolfgang Eisenreich [b,*]

[a] Working Group: Cellular Interactions of Bacterial Pathogens, Centre for Biological Threats and Special Pathogens, ZBS 2, Robert Koch Institute, Berlin, Germany
[b] Bavarian NMR Center – Structural Membrane Biochemistry, Department of Chemistry, Technische Universität München, Garching, Germany
[c] Proteomics and Spectroscopy, ZBS 6, Robert Koch Institute, Berlin, Germany

ARTICLE INFO

Keywords:
Legionella pneumophila
Acanthamoeba castellanii
Patho-metabolism
Bipartite metabolism
Stable isotope labelling
Host-pathogen interaction

ABSTRACT

The metabolism of *Legionella pneumophila* strain Paris was elucidated during different time intervals of growth within its natural host *Acanthamoeba castellanii*. For this purpose, the amoebae were supplied after bacterial infection (t =0 h) with 11 mM [U-$^{13}C_6$]glucose or 3 mM [U-$^{13}C_3$]serine, respectively, during 0−17 h, 17−25 h, or 25−27 h of incubation. At the end of these time intervals, bacterial and amoebal fractions were separated. Each of these fractions was hydrolyzed under acidic conditions. ^{13}C-Enrichments and isotopologue distributions of resulting amino acids and 3-hydroxybutyrate were determined by gas chromatography – mass spectrometry. Comparative analysis of the labelling patterns revealed the substrate preferences, metabolic pathways, and relative carbon fluxes of the intracellular bacteria and their amoebal host during the time course of the infection cycle. Generally, the bacterial infection increased the usage of exogenous glucose *via* glycolysis by *A. castellanii*. In contrast, carbon fluxes *via* the amoebal citrate cycle were not affected. During the whole infection cycle, intracellular *L. pneumophila* incorporated amino acids from their host into the bacterial proteins. However, partial bacterial *de novo* biosynthesis from exogenous ^{13}C-Ser and, at minor rates, from ^{13}C-glucose could be shown for bacterial Ala, Asp, Glu, and Gly. More specifically, the catabolic usage of Ser increased during the post-exponential phase of intracellular growth, whereas glucose was utilized by the bacteria throughout the infection cycle and not only late during infection as assumed on the basis of earlier *in vitro* experiments. The early usage of ^{13}C-glucose by the intracellular bacteria suggests that glucose availability could serve as a trigger for replication of *L. pneumophila* inside the vacuoles of host cells.

1. Introduction

Legionella pneumophila (*Lp*) is ubiquitously found in aquatic systems where it resides either in biofilms resistant to environmental stress or inside protozoa (amoebae), such as *Acanthamoeba castellanii* (*Ac*) (Rowbotham, 1980, 1986; Taylor et al., 2009; Lau et al., 2013). Infection of human alveolar macrophages can also occur mainly *via* inhalation of *Lp* containing aerosols from aquatic reservoirs (Fraser et al., 1977; Mondino et al., 2020) causing Legionnaires' disease, an atypical pneumonia accounting for 2–9 % of community acquired pneumonias (Cunha et al., 2016; Cunha and Cunha, 2017). The mechanisms of replication inside amoebae and human macrophages are thought to be highly similar. Therefore, infected amoebae are considered as a valid model for the human infection (Swart et al., 2018). Upon entry into the host cell, *Lp* builds up a compartment for replication – the *Legionella* containing vacuole (LCV) (Steiner et al., 2018). Inside this vacuole, *Lp* replicates until nutrients become limited. After this replicative phase, *Lp* leaves the LCV and changes to a mature intracellular transmissive form (MIF). These phases significantly differ in terms of morphology, gene transcription, virulence and metabolism (Byrne and Swanson, 1998; Heuner et al., 1999; Faulkner and Garduno, 2002; Brüggemann et al., 2006; Faucher et al., 2011; Price et al., 2014; Heuner and Eisenreich, 2016; Oliva et al., 2018). Generally, intracellular bacterial pathogens are characterized by a sophisticated control of their specific substrate preferences and metabolic pathways during their life cycles (Eisenreich and Heuner, 2016; Eisenreich et al., 2017; Oliva et al., 2018; Eisenreich

* Corresponding authors.
E-mail addresses: HeunerK@rki.de (K. Heuner), wolfgang.eisenreich@mytum.de (W. Eisenreich).
[1] These authors contributed equally to this work.

https://doi.org/10.1016/j.ijmm.2021.151504
Received 17 December 2020; Received in revised form 19 March 2021; Accepted 15 April 2021
Available online 19 April 2021

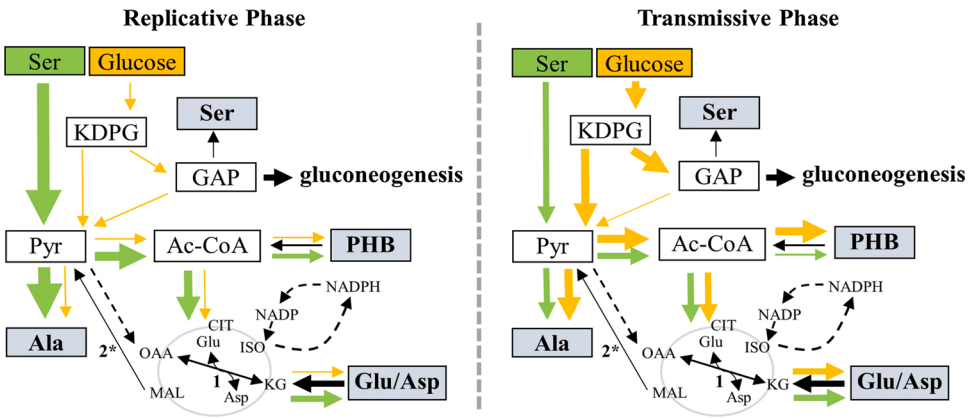

Fig. 1. Model of substrate preferences and metabolic pathways for different growth phases of *Lp* growing in AYE medium (Gillmaier et al., 2016; modified). Relative carbon fluxes are indicated by the thickness of the arrows using glucose (orange) or serine (green) as substrates. Analysed metabolites are indicated by grey boxes. The citrate cycle is indicated in grey. 1, Glu/Asp transaminase; 2*, malic enzyme (MEZ, *lpp3043* and *lpp0705*, respectively). Ac-CoA, acetyl-CoA; CIT, citrate; GAP, glyceraldehyde-3-phosphate; ISO, isocitrate; KG, α-ketoglutarate; KDPG, 2-keto-3-desoxy-6--phosphogluconate; MAL, malate; OAA, oxaloacetate; PHB, polyhydroxybutyrate; Pyr, pyruvate.

et al., 2019; Richardson, 2019; Russell et al., 2019). There is also emerging evidence that intracellular bacteria use multiple substrates orchestrated in bipartite metabolic networks (Grubmüller et al., 2014; Eisenreich and Heuner, 2016; Häuslein et al., 2016, 2017; Mehlitz et al., 2017; Best et al., 2018a, 2018b). This flexibility could enable these bacteria to rapidly adapt to the different and changing supplies of their host cells.

In line with this metabolic flexibility, substrate preferences during the respective growth phases of *Lp* growing in liquid medium were observed. During the early phase, Ser was identified as a preferred carbon substrate, whereas fatty acids, glucose and/or glycerol served as additional carbon sources during the late exponential growth phase, mainly for biosynthesis of poly-hydroxybutyrate (PHB) (Gillmaier et al., 2016; Häuslein et al., 2016) (Fig. 1).

However, the substrate usages and carbon fluxes during the infection cycle of intracellular *Lp* are only partially understood. It is established knowledge that host amino acids are among the major nutrients and are also crucial for the survival of the intracellular bacteria. Thus, a neutral amino acid transporter of the host cell (SLC1A5 in MM6 monocyte cells) as well as a bacterial threonine transporter (PhtA) were shown to be necessary for successful replication of *Lp* inside monocytes (Sauer et al., 2005; Wieland et al., 2005). In addition, some effector proteins, *i.e.* proteins which are transferred into the host cytosol using the type IV secretion system (T4SS) of *Lp* such as AnkB, catalyze poly-ubiquitinylation of host proteins. This leads to their proteasomal degradation into amino acids as welcome nutrients for intracellular *Lp* (Price et al., 2009; Lomma et al., 2010; Price et al., 2011, 2014). Moreover, the ubiquitinating enzyme SidE and the glucosyltransferase Lgt work synergistically to inhibit host translation through regulation of the mechanistic target of rapamycin complex 1 (mTORC1) (Belyi et al., 2008; De Leon et al., 2017). The upregulation of genes encoding various ABC transporters, proteases, phospholipases and amino acid permeases of intracellular *Lp* further supports the role of amino acids as nutrients (Brüggemann et al., 2006). In earlier labelling studies with *Lp* growing in amoebae, we could also confirm that host derived amino acids are directly incorporated into the bacterial proteins (Schunder et al., 2014; Eisenreich and Heuner, 2016; Häuslein et al., 2016).

The role of glucose as a potential nutrient for intracellular *Lp* is still obscure, although several earlier findings already pointed towards the importance of the carbohydrate during intracellular survival (Eylert et al., 2010; Harada et al., 2010; Herrmann et al., 2011; Gillmaier et al., 2016). Indeed, the ability of glucose uptake by *Legionella* was shown to be necessary for intracellular replication, although it did not affect bacterial growth *in vitro* (Best et al., 2018a, 2018b). Amylases and enzymes of the Entner Doudoroff pathway (ED pathway) catalyzing glucose degradation were also reported to be important for intracellular replication (Eylert et al., 2010; Harada et al., 2010; Häuslein et al., 2016; Manske et al., 2016; Häuslein et al., 2017; Best et al., 2018a, 2018b; Levanova et al., 2019). More specifically, the Δ*lamB* amylase mutant was severely attenuated in intra-pulmonary proliferation in mice (Best et al., 2018a, 2018b) and the *zwf* gene encoding glucose-6-phosphate dehydrogenase in the ED pathway for glucose usage was induced during growth in amoebae, but not in human macrophages (Brüggemann et al., 2006; Faucher et al., 2011). The Δ*zwf* mutant showed reduced growth in both amoebae and macrophages (Eylert et al., 2010; Harada et al., 2010). In line with these findings, myo-inositol derived from glucose metabolism accumulated inside the LCV and enhanced intracellular growth (Manske et al., 2016).

The effect of bacterial infections upon the metabolism of their host organisms has also hardly been investigated. Before infection by bacterial pathogens, the typical metabolic state of most host cells does not meet the extensive need for nutrients and energy by the invasive bacteria. To increase the supply of nutrients, energy, and metabolites for replication inside their host cells, most intracellular bacteria have therefore developed smart mechanisms to reprogram the metabolism of their hosts (Price et al., 2014; Best and Abu Kwaik, 2019; Eisenreich et al., 2019). For example, the uptake and metabolism of glucose is strongly increased in primary murine or human cells as a response upon infection by intracellular *Listeria monocytogenes* (Krawczyk et al., 2010; Gillmaier et al., 2012). In *Dictyostelium discoideum*, another amoebal host for *Lp*, infection with *Lp* downregulated genes involved in defense reactions against the infection, but upregulated many genes encoding enzymes for general metabolic functions (*e.g.* protein biosynthesis and carbohydrate metabolism) and the stress response (Farbrother et al., 2006). Experiments with *Acanthamoeba polyphaga* as a host revealed increased lactate secretion and higher levels of glucose-6-phosphate in the amoebal cytosol during infection dependent on the T4SS of *Lp*, which could point at a stimulation of glycolysis triggered by effector proteins (Price et al., 2020).

To reveal the substrate usages and the core energy metabolism of *Lp* for different time periods of the infection and to elucidate impacts of the infection upon the host metabolism, we here took advantage of ^{13}C-labelling experiments. Specifically, [U-$^{13}C_6$]glucose or [U-$^{13}C_3$]serine were supplied to infected *Ac* during various intervals of the infection cycle. This technique provided direct insights into the relative carbon fluxes and was therefore qualified to determine differential substrate usages and metabolic pathways in the infection cycle. Using the same setting, we also analysed the Δ*zwf* mutant of *Lp* to better understand the role of glucose during intracellular growth. Since the protein encoded by the *zwf* gene catalyzes the entry reaction of the ED pathway, the main route for glucose usage in *Lp* (Eylert et al., 2010; Harada et al., 2010), the Δ*zwf* mutant strain was especially useful to clarify the importance of glucose metabolism by intracellular *Lp*.

2. Materials and methods

2.1. Strains, growth conditions, media, and buffer

L. pneumophila Paris wild type (in the following *Lp*) was used in this study (Cazalet et al., 2004). For comparison, the following mutant strains were studied by *in vivo* infection assays: *L. pneumophila* Paris *zwf* (*lpp0483*, glucose-6-phosphate-dehydrogenase) (Eylert et al., 2010) and *L. pneumophila* Corby *fliA* (Heuner et al., 2002). *Lp* was grown in yeast extract broth buffered with *N*-(2-acetoamido)-2-aminoethanesulfonic acid (AYE) consisting of 10 g of *N*-(2-acetoamido)-2-aminoethanesulfonic acid, 10 g of yeast extract, 0.4 g of *L*-Cys, and 0.25 g of ferric pyrophosphate per L (adjusted to pH 6.8 with 3 M KOH and sterile filtrated) at 37 °C with agitation at 250 rpm or on buffered charcoal-yeast extract (BCYE) agar for 3 days at 37 °C. Bacterial growth in broth was monitored by determining the A_{600} with a Thermo Scientific GENESYS 10 Bio spectrophotometer (VWR, Darmstadt, Germany). When appropriate, media were supplemented with kanamycin at final concentrations of 8 or 40 μg/mL, respectively. For cultivation of *Lp* on agar plates, kanamycin was used at a final concentration of 12.5 μg/mL.

A. castellanii ATCC 30010 (in the following *Ac*) was cultured in PYG712 medium (2 % proteose peptone, 0.1 % yeast extract, 0.1 M glucose, 4 mM $MgSO_4$ x 7 H_2O, 0.4 M $CaCl_2$ x 2 H_2O, 0.1 % sodium citrate dihydrate, 0.05 mM $Fe(NH_4)_2(SO_4)_2$ x 6 H_2O, 2.5 mM NaH_2PO_4, and 2.5 mM K_2HPO_4) at 20 °C. The so-called *Acanthamoeba* (Ac) buffer was PYG712 medium without peptone, yeast extract, and glucose.

2.2. Intracellular replication and determination of time points

Intracellular replication was monitored by lysing infected amoebae at different time points followed by plating the supernatant onto BCYE agar plates and determination of the CFUs. Infection was also observed microscopically by counting intact amoebae and "rotating vacuoles" (Rowbotham, 1986) as a result from motile *Lp* inside vacuoles due to the formation of flagellae.

2.3. ^{13}C-Labelling experiments of Lp growing in Ac

Ac was cultivated in 12 cell culture flasks (175 cm^2) (Heuner et al., 2019). A volume of 50 mL PYG712 medium was inoculated (1:10) and incubated for 3 days at room temperature. The adhered amoebae were washed two times by gently shaking the flask with 10 mL of Ac buffer and then incubated for 2 h at 37 °C in 50 ml of fresh Ac buffer. *Lp* grown on a BCYE agar plate for 3 days was diluted in Ac buffer. The suspension was adjusted to an A_{600} of 1, and 1 mL of the suspension (about 10^9 bacteria) per flask was used for infection resulting in a MOI of about 100. After 2 h at 37 °C, all extracellular bacteria were removed by washing with 10 mL Ac buffer and by adding 50 μg/mL gentamicin for 1 h at 37 °C. Gentamicin was removed by washing with 10 mL Ac buffer. Infected amoebae were incubated in 50 mL fresh Ac buffer for given time periods. For ^{13}C-labelling, the infected amoebae were incubated in Ac buffer supplemented with 11 mM [U-$^{13}C_6$]glucose or 3 mM [U-$^{13}C_3$]serine during time periods of 0−17 h, 17−25 h and 25−27 h after infection (t = 0) at 37 °C, respectively. Additionally, infected amoeba were incubated in Ac buffer supplemented with 55 mM [U-$^{13}C_6$]glucose during the time intervals 17−25 h and 25−27 h after infection. Cells were harvested at the end of the given time interval and an aliquot was plated out on LB agar plates. The plates were incubated for 24 h to exclude the possibility of contaminations. The infected amoebae were frozen for at least 2 h at −80 °C, thawed in a 37 °C water bath and vortexed for 20 s. Successful lysis was monitored microscopically. Differential centrifugation allowed separation of unlysed amoebae and high-density cellular components (fraction 1, F1), *Lp* (fraction 2, F2), and the cytosolic proteins of *Ac* (fraction 3, F3) using the protocol as follows. The suspension was first centrifuged at 600*g* and 4 °C for 15 min. The pellet containing F1 was washed three times with Ac buffer. The supernatant was then transferred to a new tube and centrifuged at 3600*g* and 4 °C for 15 min. The resulting pellet (F2) was washed two times in distilled water, and the supernatant F3 was filtrated through a 0.22 μm pore filter to exclude contaminating bacteria. All three fractions were autoclaved at 120 °C for 20 min and stored at −20 °C until work-up for GC–MS analysis.

2.4. SDS PAGE and immunoblotting

SDS-PAGE and Western blotting were done as described elsewhere (Laemmli, 1970; Towbin et al., 1979). Fractions F1–F3 obtained from four flasks of infected *Ac* were dissolved in 200 μL of distilled water. For SDS-PAGE, 10 μL of each fraction were resuspended with 4 μL of Roti-Load denaturating sample buffer, boiled for 10 min, and loaded on a 12 % SDS-polyacrylamide gel. Synthesis of the flagella was detected using polyclonal anti-FlaA antiserum diluted in 1 % milk and tris-buffered saline (1:1000). The horseradish peroxidase-conjugated goat α-rabbit IgG antibody was used as the secondary antibody (1:1000) (Dianova, Hamburg, Germany). Lysates of stationary *Lp* WT and the mutant Δ*fliA*, unable to express flagella, served as a control. FlaA was visualized using commercially available Pierce enhanced luminol-based chemiluminescent (ECL) Western blotting substrate and ECL detection solution (Thermo Fisher Scientific), which was exposed to X-ray films.

2.5. Fourier-transform infrared absorption spectroscopy of whole Lp cells to quantify poly-hydroxybutyrate (PHB)

F2 was diluted in 1 μL distilled water. Fourier-transform infrared (FT-IR) absorption spectra were obtained using a FT-IR microscope IR Scope II, coupled to an IFS28/B spectrometer (Bruker Optics, Ettlingen, Germany) and equipped with a broadband mercury–cadmium–telluride (MCT)-detector, and a motorized x,y stage. The measurements were performed in transmission/absorbance mode and the parameters used were: 6 cm^{-1} nominal spectral resolution, zero-filling-factor of 4, and a Blackman–Harris-Three-Term apodization function prior to Fourier transformation. All spectra were collected with a 15× Cassegrain-objective and were acquired under stable measurement and nearly free of water vapour conditions in the spectral region between 600 cm^{-1} and 4000 cm^{-1}. The measurements of samples were performed selecting aperture diameters of 50 μm and averaging 64 interferograms. Spectral data processing was performed using the software OPUS 5.5 for Windows XP Professional (Bruker Optics, Ettlingen, Germany).

2.6. Measurement of glycogen in Ac by FT-IR spectroscopy

Ac cells were cultivated in 175 cm^2 flasks in PYG medium for 8 days. Co-cultivation with *Lp* was carried out as described above or cells were left uninfected. About 10^7 cells were harvested 17, 25 or 27 h after infection and frozen for at least 2 h at −80 °C and thawed afterwards followed by centrifugation at 3600*g* for 15 min at 4 °C. Cells were washed with 0.9 % NaCl. The pellet was resuspended in 100 μL H_2O_{dd} and applied onto a ZnSe sample holder and dried to a film in a desiccator under moderate vacuum (0.9 bar) over P_4O_{10} (Sicapent, Merck) for 30 min. The sample holder was sealed with a KBr cover plate. FT-IR spectra for glycogen were measured as described before for PHB (Gillmaier et al., 2016). Background spectra were collected from an empty position of the ZnSe sample holder. Spectral data processing was performed using the software OPUS 5.5 for Windows XP Professional (Bruker Optics, Ettlingen, Germany).

2.7. Sample preparation for ^{13}C-isotopologue analysis of proteinogenic amino acids and 3-hydroxybutyrate

Each of F2- and F3-fractions was dried by lyophilization. Analysis of protein bound amino acids and PHB in the form of 3-hydroxybutyrate was basically done as described earlier (Eylert et al., 2008; Schunder

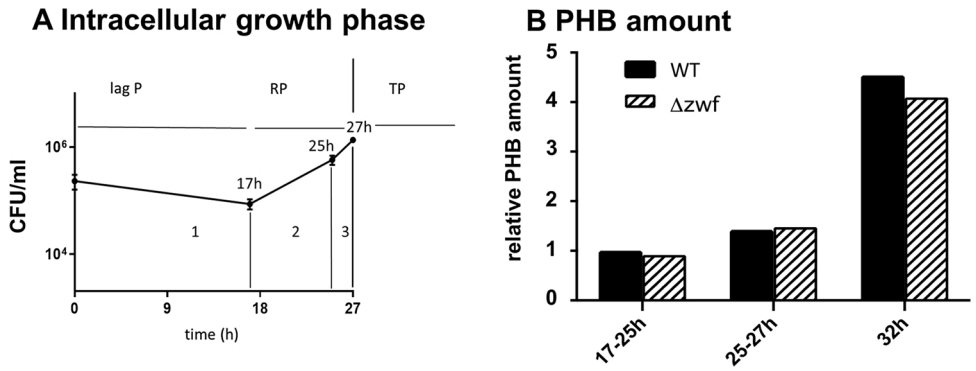

Fig. 2. Growth phase dependent analysis of PHB amounts during intracellular growth of *Lp*. A. Analysis of CFU during intracellular replication in *Ac* (n = 2). Lag P, lag-phase; RP, replicative phase; TP, transmissive phase. B. Relative amounts of PHB in *Lp* WT and the Δzwf mutant as measured by FT-IR analysis.

et al., 2014). In brief, about 2 mg of the dried fractions were subjected to acidic hydrolysis (0.5 mL of 6 M HCl, 15 h, 105 °C). Afterwards, cation exchange chromatography using Dowex 50 W X8 (7 × 10 mm; 200–400 mesh, 34−74 µm, H+-form, Alfa Aesar) yielded an aqueous eluate containing 3-hydroxybutyrate and an alkaline eluate containing amino acids. For derivatization of the amino acid-fraction, the alkaline eluate was dried under a stream of nitrogen at 70 °C and the residue was mixed with 50 µL of anhydrous acetonitrile and 50 µL of *N*-methyl--*N*-*tert*-butyldimethylsilyltrifluoroacetamide (Sigma Aldrich). The mixture was incubated at 70 °C for 30 min. For derivatization of 3-hydroxybutyrate, the water eluate was dried under a stream of nitrogen at 70 °C and the residue was mixed with 100 µL of *N*-methyl--*N*-trimethylsilyl-trifluoroacetamide (Sigma Aldrich). This mixture was incubated at 40 °C for 90 min while shaking with 110 rpm.

2.8. GC–MS parameters for ^{13}C-isotopologue analysis

In general, the silylated derivatives were analysed using a Shimadzu GC–MS (GCMS-QP 2010 Plus spectrometer, Shimadzu, Duisburg, Germany) as described earlier (Häuslein et al., 2016). For GC–MS analysis of silylated amino acids, the column was heated to 150 °C and kept for 3 min. A gradient of 7 °C/min was then applied until a final temperature of 280 °C, which was held for 3 min. For GC–MS analysis of silylated 3-hydroxybutyrate, the column was developed at 70 °C for 3 min and then with a temperature gradient of 10 °C/min to a final temperature of 150 °C. This was followed by a temperature gradient of 50 °C/min to a final temperature of 280 °C, which was held for 3 min.

2.9. Data evaluation and statistics

GC–MS data evaluation was performed using Shimadzu LabSolution software V4.20. ^{13}C-Excess values were calculated using an Excel-based in-house software based on an earlier procedure (Lee et al., 1991). Labelling experiments were typically performed twice to afford two biological replicates. GC–MS measurements were performed in triplicates for each sample to demonstrate the robustness of the measurements.

3. Results and discussion

3.1. Establishing a growth-phase dependent infection model of Lp in Ac

The major object of this study was to determine the dynamics of substrate usages and metabolic pathways during the full growth cycle of *Lp* in amoebae. In earlier studies of intracellular *Lp*, we supplied [U-$^{13}C_6$]glucose to *Ac* before infection (t =0 h), which gave some insights into *Lp* metabolism during the whole infection cycle (Heuner et al., 2019). To achieve time resolution during the infection cycle, we now selected three different time intervals 1–3 (see Fig. 2A), where we

Table 1
Growth phase dependent characterisation of intracellularly growing *Lp*. Replication of *Lp* was determined by CFU. Flagellin expression was determined in a Western blot using an α-flagellin-antiserum (data not shown). Rotating vacuoles, which are a result of flagellated *Lp* moving inside the vacuole, and lysed amoeba were monitored and counted microscopically. PHB was determined by FT-IR analysis. Data are based on two biological replicates.

	17 h after infection	25 h after infection	27 h after infection	32 h after infection
Lp replication	+	++	++	n.d.
Lp flagellation*	–	+	++	n.d.
"Rotating vacuoles"	–	1.3 %	2.5 %	0.8 %
Lysed amoeba	–	4.2 %	15 %	50.2 %
Relative PHB amount	–	+	+	+++

n.d., not determined.
* Indirectly determined by the detection of flagellin protein.

added ^{13}C-glucose or alternatively ^{13}C-Ser to the infected amoebae. Western blot analysis using an anti-flagellin antiserum and microscopic analysis of the fraction of "rotating vacuoles" as an indication of flagellated *Lp* moving inside the vacuoles (Table 1) (Rowbotham, 1986) were used to assess intracellular motility of *Lp*. These results suggested that the time interval 1 (0−17 h after the infection of the amoebae) represented the lag phase of *Lp* and the beginning of intracellular replication. During this phase, the bacteria were non-flagellated and accordingly "rotating vacuoles" were not detected. The time interval 2 (17−25 h) represented the main peak of the replicative phase (RP), where *Lp* started to express the flagellum towards the 25 h-time point. However, still only a small fraction of amoebae (< 2 %, Table 1) contained "rotating vacuoles" at this time. During time interval 3 (25−27 h), the bacteria rapidly reached the post-exponential phase (PE), in which most *Lp* became flagellated and motile. A minor fraction of amoebae (about 15 %, Table 1) had already been lysed at the 27 h-time point. During this late interval, the bacteria synthesized high amounts of PHB (Fig. 2B). The subsequent transmissive phase (TP) (stationary phase, 27−32 h, Table 1) showed the presence of huge amounts of extracellular bacteria (> 50 % at 32 h). Although the synthesis of PHB reached its maximum during this phase (Fig. 2B), this time interval was not further studied by ^{13}C-profiling since the respective labelling data would largely reflect the fraction of extracellular *Lp*.

After harvest at the end of the indicated time intervals, the bacteria (highly enriched in the F2 fraction) were separated from the cytosolic amoebal proteins (F3), hydrolysed, converted into volatile silyl derivatives, and subjected to GC–MS analysis following established protocols (Schunder et al., 2014; Heuner et al., 2019). In both fractions, the ^{13}C-labelling patterns of 14 amino acids could be determined (Supplemental Tables 1–24). The differential ^{13}C-excess values of these amino

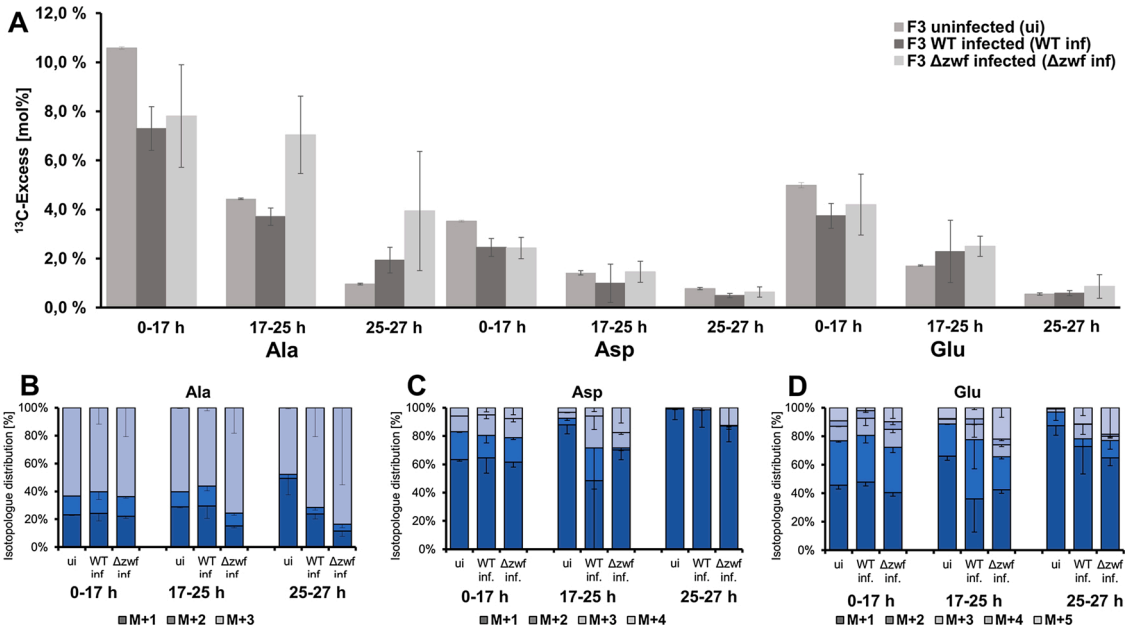

Fig. 3. Effects of the *Lp*-infection upon amoebal metabolism. (A) ^{13}C-Enrichments in mol% of amino acids from amoebal proteins, *i.e.* from the F3 fraction, in uninfected *Ac* and after infection with *Lp* WT or the Δ*zwf* mutant in the experiment with [U-$^{13}C_6$]glucose. (B–D) Relative isotopologue compositions of labelled Ala, Asp and Glu in the experiment with [U-$^{13}C_6$]glucose. M + X indicates an isotopologue containing X ^{13}C-atoms. Error bars indicate standard deviations based on two biological replicates (n = 2) with three technical replicates each, except for the experiment with uninfected amoeba, which are based on one biological replicate (n = 1) with three technical replicates.

acids with their relative fractions of specific isotopologues (*i.e.* molecules containing a certain number of ^{13}C-atoms were now taken as the basis to derive key metabolic pathways of the intracellular bacteria and their host cells. Moreover, the labelling patterns of silylated 3-hydroxybutyrate resulting from hydrolysis of bacterial PHB in F2 allowed to specifically analyse the metabolism of the storage compound (Supplemental Tables 25–33).

3.2. Amoebal glycolysis is stimulated by the bacterial infection

By comparing the labelling patterns of amino acids from *Lp*-infected amoebae (F3) with the corresponding ones from uninfected *Ac*, we could study the impact of the *Legionella* infection upon the amoebal metabolism (Fig. 3). Here, we focused on the ^{13}C-patterns of Ala, since this amino acid directly derives from pyruvate, the product of glycolysis (Fig. 3B). Similarly, Asp was a useful reporter since it is the amination product of the TCA cycle-intermediate oxaloacetate, and is therefore a valid reporter for fluxes *via* the TCA cycle as well as for pyruvate carboxylation forming oxaloacetate (Fig. 3C). Following the same methodology, Glu was taken as the reporter for the TCA cycle-intermediate α-ketoglutarate, and thus also reflects fluxes *via* the TCA cycle (Fig. 3D).

In the experiment with [U-$^{13}C_6$]glucose, Ala, Asp, and Glu from the amoebal fraction (F3) displayed significant ^{13}C-excess values (1–10 %) for uninfected as well as for infected amoebae during the three time periods in our experiments (Fig. 3A, Supplemental Tables 1, 3, 5, 7, 9, 11, 34). Generally, these values decreased towards the latter time periods, probably influenced by the shorter time spans. As another reason, the observed degradation of glycogen in amoebae over time (see FT-IR analysis, SI Fig. 1) led to the release of unlabelled glucose, which may have caused dilution of ^{13}C-excess in free (available) glucose, thus also resulting in lower ^{13}C-enrichments of amino acids during the late time periods. Importantly, however, this decrease was less pronounced for Ala (reporter for glycolytic flux) from the infected cells and, as a noticeable exception, even reversed during the third period, when comparing infected with uninfected cells (Fig. 3A). This could be taken as clear evidence that amoebal glycolysis was stimulated by the bacterial infection with increasing rates towards the replicative phase of intracellular *Lp*.

In line with this conclusion, ^{13}C-excess values of Ala in F3 were higher in amoebae infected by the Δ*zwf* mutant strain as compared with amoebae infected with *Lp* WT (Fig. 3A). Obviously, more ^{13}C-glucose was available for amoebal glycolysis in the experiment with the mutant, since the Δ*zwf* strain was unable to retrieve ^{13}C-glucose from the host for bacterial metabolism (see below). Thus, all these observations indicated that the bacterial infection stimulated the formation of ^{13}C-Ala *via* conversion of ^{13}C-glucose into ^{13}C-pyruvate followed by transamination to ^{13}C-Ala. Differences in the relative isotopologue fractions became also evident in the labelling patterns of Ala from F3 (Fig. 3B, Supplemental Tables 2, 4, 6, 8, 10, 12, 35). As expected, the ^{13}C-profile of amoebal Ala was indicative for [U-$^{13}C_6$]glucose degradation *via* glycolysis mainly resulting in the $^{13}C_3$-isotopologue (*i.e.* Ala carrying three ^{13}C-atoms, also denoted as M + 3). The M + 3 fraction was highest in Ala from the infected amoebae of the late time interval, which again corroborated that amoebal glycolysis was stimulated during the bacterial infection. This effect was stronger when the amoebae were infected with the Δ*zwf* mutant of *Lp* (Fig. 3B). Interestingly, the detected increase of glycolytic flux of *Lp*-infected *Ac* was in line with the previously reported upregulation of genes involved in glucose homeostasis and cell wall catabolism of *Lp*-infected *Dictyostelium* (Farbrother et al., 2006) and upregulation of glycolysis in the amoeba *A. polyphaga* due to the T4SS of *Lp* (Price et al., 2020).

From the unchanged labelling data for Asp and Glu from F3 of infected *vs*. uninfected *Ac*, it could be concluded that the amoebal TCA cycle and glutaminolysis were less or not affected by the bacterial infection (Fig. 3A, C, D; Supplemental Tables 2, 4, 6, 8, 10, 12, 35). Not surprisingly, the isotopologue compositions of Asp and Glu reflected their origin *via* the TCA cycle and related anaplerotic reactions but these patterns were almost identical for uninfected and infected *Ac* (Fig. 3C, D).

3.3. The dynamics of PHB metabolism in intracellular Lp

The polymerisation and depolymerisation of PHB by intracellular *Lp*

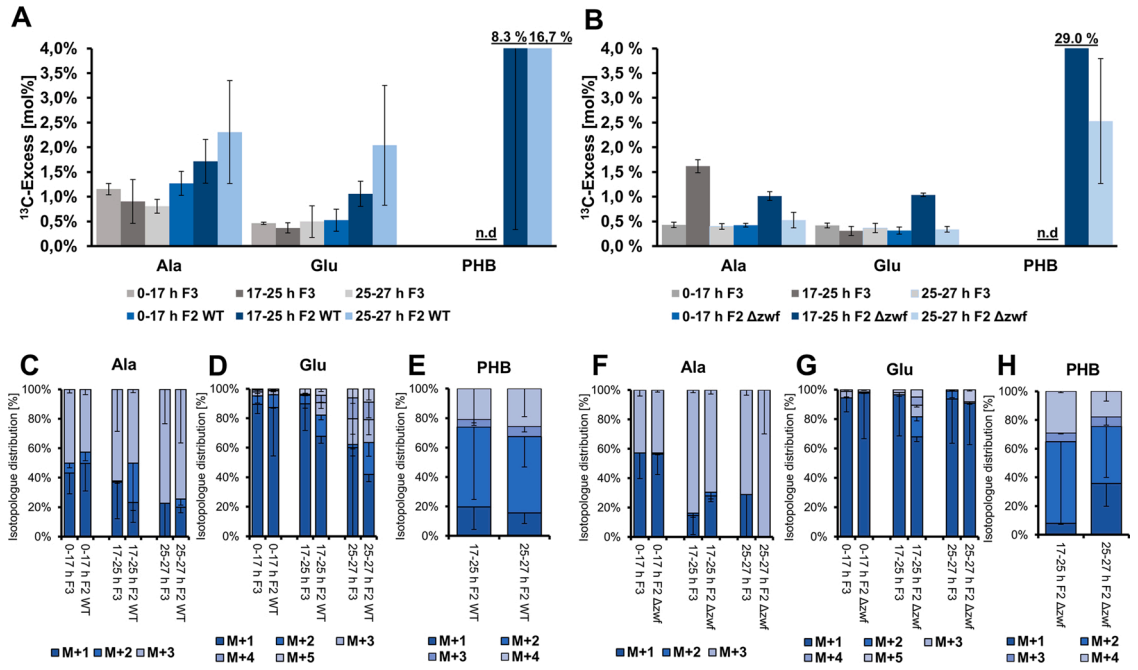

Fig. 4. Key data from the labelling experiment with [U-$^{13}C_3$]serine. Analysis of the ^{13}C-patterns in amino acids in comparison of the different growth phases of intracellular *Lp* WT and its Δ*zwf* mutant. ^{13}C-Excess in mol% of amino acids in *Ac* (from the F3 fractions) and amino acids and 3-hydroxybutyrate (from the respective F2 fractions) in *Lp* WT (A) and its Δ*zwf* mutant (B). Isotopologue profiles of the respective compounds from *Lp* WT (C–E) and its Δ*zwf* mutant (F–H). M + X indicates the isotopologue with X ^{13}C-atoms incorporated into the respective compound. Error bars indicate standard deviations based on two biological replicates (n = 2) with three technical replicates each, except for the data with ^{13}C-serine and *Lp* Δ*zwf*, which is based on one biological experiment (n = 1) with three technical replicates. n. d., not determined.

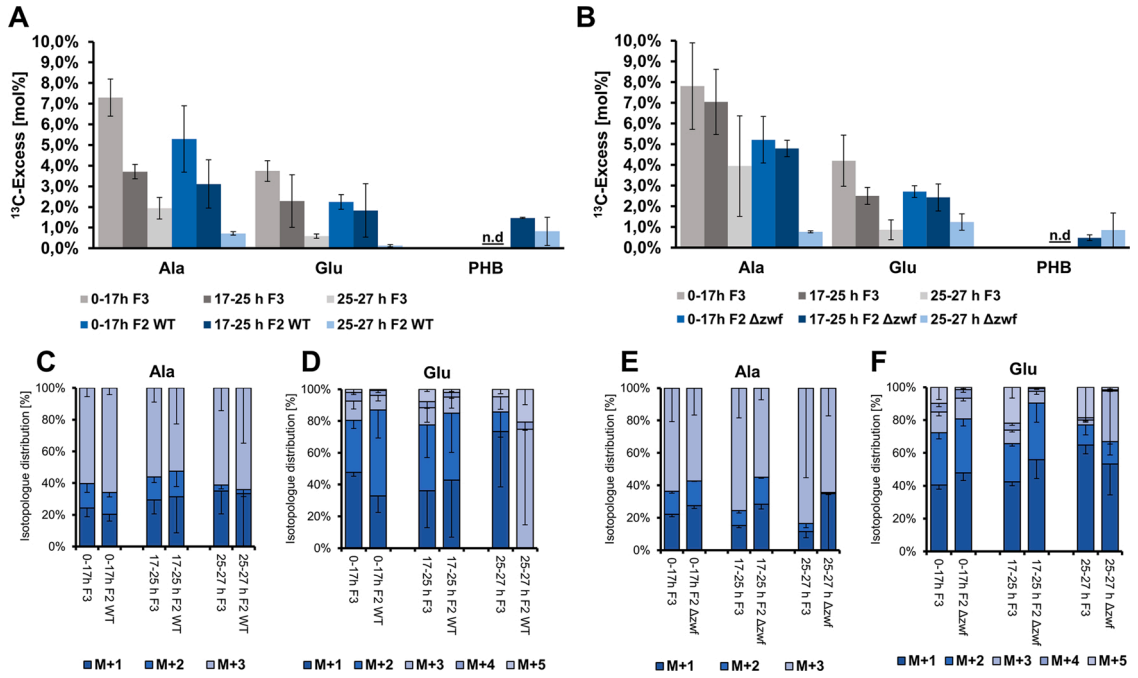

Fig. 5. Key data from the labelling experiment with [U-$^{13}C_6$]glucose. Analysis of the ^{13}C-patterns in amino acids in comparison of the different growth phases of intracellular *Lp* WT and its Δ*zwf* mutant. ^{13}C-Excess in mol% of amino acids in *Ac* (from the F3 fractions) and amino acids and 3-hydroxybutyrate (from the respective F2 fractions) in *Lp* WT (A) and its Δ*zwf* mutant (B). Isotopologue profiles of the respective compounds from *Lp* WT (C, D) and its Δ*zwf* mutant (E, F). M + X indicates the isotopologue with X ^{13}C-atoms incorporated into the respective compound. Error bars indicate standard deviations based on two biological replicates (n = 2) with three technical replicates each. n.d., not determined.

has not yet been investigated in detail. It seemed as if PHB synthesis by intracellular *Lp* is higher than by bacteria grown in medium, and that PHB, generated in the MIF inside amoebae, is important for subsequent extracellular survival of *Lp* (Rowbotham, 1986; James et al., 1999; Garduno et al., 2002; Robertson et al., 2014).

Based on the observed ^{13}C values and patterns of 3-hydroxybutyrate

isolated from the hydrolysed F2 fraction (as the proxy for bacterial PHB) either starting from ^{13}C-glucose or ^{13}C-serine in our setting, it was obvious that 3-hydroxybutyrate formation not only occurs late in the life cycle of intracellular *Lp*, but already during the first growth phase (Figs. 4A, 5 A). Then, polymerisation of 3-hydroxybutyrate into PHB increased during the late replicative phase, as reflected by the higher amounts of cellular PHB detected by FT-IR spectrometry (Fig. 2B). During the late growth phase, incorporation from ^{13}C-serine into 3-hydroxybutyrate further increased (Fig. 4A). In the transmissive phase, PHB amounts also increased (Fig. 2B, 32 h). ^{13}C-Flux from glucose into PHB slightly decreased during the transmissive phase (Fig. 5A, B, SI Fig. 2). Thus, PHB synthesis seemed to peak very shortly before lysis of the host cell. The previously reported negative effect of the Δ*zwf* mutant strain on ^{13}C-flux from glucose into PHB synthesis under *in vitro* conditions (Gillmaier et al., 2016) was also detected during intracellular growth in *Ac* (SI Fig. 2, Supplemental Table 36). However, the amount of PHB was nearly similar in *Lp* WT and the Δ*zwf* mutant (Fig. 2B), which was partly at odds to our earlier finding under *in vitro* conditions, where the *zwf* mutant strain synthesized less PHB (51–68 %) (Gillmaier et al., 2016). Other substrates such as fatty acids (Häuslein et al., 2017), leucine (Heuner, unpublished results; Tesh et al., 1983), as well as further genes, like those encoding for ketothiolase (*lpp1788*), the PHB polymerase (*lpp650*), the alternative fatty acid degradation pathway (*lpp0931-33*) (Gillmaier et al., 2016), and the *bdhA* (PHB dehydrogenase) (Aurass et al., 2009) have been shown to be involved in the metabolism of PHB at different efficiencies when comparing intracellular *Lp* with *Lp* grown in medium. The complex interplay of these factors under intracellular conditions could explain the apparent discrepancies between the *in vivo* and *in vitro* results.

3.4. Differential usage of Ser during the infection cycle of Lp

In the experiment with [U-$^{13}C_3$]serine, the ^{13}C-enrichments of Ala, Glu and 3-hydroxybutyrate from *Lp* (F2 fraction) increased with the duration of the experiment (Fig. 4A, B, Supplemental Tables 13, 15, 17, 19, 21, 23, 29, 31). Labelled Ala mostly consisted of the M + 3-isotopologue (Fig. 4C, F, Supplemental Tables 14, 16, 18, 20, 22, 24, 30, 32), while the isotopologue profile of Glu comprised a diverse pattern of isotopologues arising through multiple rounds of the TCA cycle (Fig. 4D, G). The labelling pattern of 3-hydroxybutyrate reflected the incorporation of one or two evenly or unevenly labelled acetyl-CoA precursor molecules (Fig. 4E, H, Supplemental Tables 30, 33). These findings could be taken as evidence that ^{13}C-Ser or a closely related compound was transferred from the host into the LCV and converted by the bacterial metabolism into pyruvate, acetyl-CoA, and α-ketoglutarate. These metabolites were then used at increasing rates during the experiment as precursors for Ala, 3-hydroxybutyrate (PHB), and Glu biosynthesis, respectively. This conclusion was especially underlined by the ^{13}C-data of 3-hydroxybutyrate. Its ^{13}C-excess increased from 8.3 % during the second time interval up to 16.7 % towards the post-exponential phase in *Lp* WT (Fig. 4A).

Notably, the finding that Ser serves as a carbon source for intracellular *Lp* at increasing rates during the late growth phase was partially in contrast to data from earlier *in vitro* experiments where Ser was the preferred carbon substrate during the early phase of growth (Gillmaier et al., 2016). However, this apparent discrepancy could be explained by the induction of a serine transport protein (Lpp2269) during the transmissive phase of intracellular growth (Brüggemann et al., 2006) resulting in the increased usage of ^{13}C-Ser during the late phase of the intracellular life cycle.

3.5. Differential usage of glucose during the infection cycle of Lp

In the experiment with [U-$^{13}C_6$]glucose, the detected ^{13}C-excess in 3-hydroxybutyrate from the F2 fraction (as the proxy for *Lp*-specific PHB) again indicated that the external ^{13}C-glucose was transported into the LCV where it was used as a carbon source for bacterial metabolism (Fig. 5A, B, Supplemental Tables 1, 3, 5, 7, 9, 11, 25, 27). To get more insight into the pathways for glucose usage by intracellular *Lp*, we again focussed on the labelling patterns of Ala from F2 (reporter for the bacterial ED pathway), Glu, Asp (reporters for the bacterial TCA cycle) (Fig. 5C–F, Supplemental Tables 2, 4, 6, 8, 10, 12, 26, 28) and, additionally Gly, because its biosynthesis depends on NADPH, which is produced *via* the oxidative branch of the bacterial pentose phosphate pathway (PPP). However, the interpretation of the ^{13}C-patterns in Ala, Asp, Glu and Gly was complicated by the fact that these amino acids were also efficiently formed by the host metabolism from the glucose supply (Schunder et al., 2014) and partly taken up by *Lp* already in ^{13}C-labelled form from their host. As a general prerequisite for proper data interpretation, it was therefore important to compare the ^{13}C-patterns of bacterial amino acids (F2 fraction) with the ^{13}C-patterns of the respective host amino acids (F3 fraction). Moreover, data interpretation was facilitated by control experiments using the Δ*zwf* mutant of *Lp* hampered in glucose metabolism (Eylert et al., 2010).

3.5.1. Glucose usage during the early phase of intracellular growth

During the first time interval (0−17 h) of the experiment with [U-$^{13}C_6$]glucose, when the bacteria established the LCV and began to replicate, the relative fractions of M + 3 and M + 2 isotopologues in Ala and Glu, respectively, were significantly higher in the bacterial fraction F2 as compared to the host fraction F3 (Fig. 5C, D). Notably, the overall ^{13}C-excess values of Ala and Glu from the intracellular bacteria were also highest during this period (Fig. 5A). These findings indicated that, already during the early period, ^{13}C-glucose contributed to the *de novo* biosynthesis of the bacterial amino acids, which was again partly in contrast to the earlier findings for *Lp* grown under *in vitro* conditions, where glucose was barely among the carbon substrates during the early replicative phase of *Lp* (Eylert et al., 2010).

However, the early usage of glucose by intracellular *Lp* was also clearly confirmed by the corresponding *in vivo* labelling experiment with the Δ*zwf* mutant of *Lp*. In sharp contrast to the corresponding ^{13}C-data from intracellular *Lp* WT, the fractions of M + 3 and M + 2 in Ala and Glu, respectively, from the mutant were significantly lower during this first time interval (0−17 h) (Fig. 5E, F). Indeed, this provided firm evidence that external [U-$^{13}C_6$]glucose could not be utilized by the mutant and that mainly (or only) labelled Ala und Glu from the host were incorporated into bacterial protein as already seen in our earlier experiments with ^{13}C-prelabelled amoebae (Schunder et al., 2014).

Importantly, the finding that host glucose was utilized during the early infection period may indicate that the carbohydrate could serve as a signal that – besides other factors – triggers the transition from the lag-phase to the replicative phase, similar to amino acid starvation controlling the shift from the replicative phase to the transmissive phase in *Lp* (Hammer and Swanson, 1999; Sauer et al., 2005). In support of this hypothesis, *Lp* exhibits a homolog of GidA (*lpp2948*), which in *Escherichia coli* encodes for a glucose-sensitive division protein, and which is also involved in the pathogenicity of various pathogens (Sha et al., 2004; Cho and Caparon, 2008; Gupta et al., 2009; Rehl et al., 2013). Further studies are required to unravel the potentially regulatory role of glucose and GidA during intracellular growth of *Lp*.

3.5.2. Glucose usage during the later phases of intracellular growth

During the later periods of the experiment (17−25 h, 25−27 h), the isotopologue profiles of host and bacterial amino acids in *Lp* WT as well as in the Δ*zwf* mutant became more and more similar, indicating that other substrates may have competed as efficient precursors for the reporter amino acids (Fig. 5C–F). However, the experiment with the Δ*zwf* mutant strain of *Lp* suggested that the bacteria replicating inside the vacuole still had access to the externally supplied glucose also during the late phase. This conclusion was especially underlined by comparing the ratios of ^{13}C-excess values (ratios F2:F3) for Ala, Asp and Gly (SI Fig. 3). In the late phase, these ratios were significantly higher for the *Lp* WT in

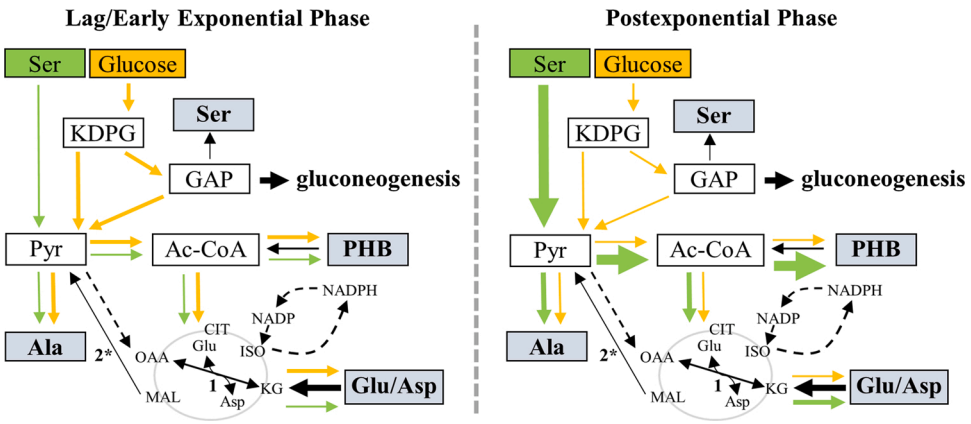

Fig. 6. Model of substrate preferences and metabolic pathways for different growth phases of *Lp* growing inside *Ac* (Gillmaier et al., 2016; modified). Relative carbon fluxes are indicated by the thickness of the arrows starting from glucose (orange) or serine (green) as substrates. Analysed metabolites are indicated by grey boxes. The citrate cycle is indicated in grey. 1, Glu/Asp transaminase; 2*, malic enzyme (MEZ, *lpp3043* and *lpp0705*, respectively). Ac-CoA, acetyl-CoA; CIT, citrate; GAP, glyceraldehyde-3-phosphate; ISO, isocitrate; KG, α-ketoglutarate; KDPG, 2-keto-3-desoxy-6-phosphogluconate MAL, malate; OAA, oxaloacetate; PHB, polyhydroxybutyrate; Pyr, pyruvate.

comparison to the ratios for the Δ*zwf* mutant. Indeed, higher ratios for *Lp* WT indicated their metabolic usage of ^{13}C-glucose in contrast to the mutant strain, which was unable to utilize glucose *via* the ED pathway. In conclusion, ^{13}C-glucose was metabolized/cycled during the late phase at higher efficiencies in the WT (thus increasing the values for F2 for the WT) than in the Δ*zwf* mutant. In addition, using ^{13}C-glucose as a substrate for *Lp* WT, the M + 1 fraction in Gly (F2) was higher than the M + 2 fraction with an increasing trend over time, which is in contrast to the host (F3), but which is in accordance with in-medium grown *Lp*. This indicated that Gly was synthesized from the ^{13}C-supply by intracellular *Lp* itself leading to the observed differences in the isotopologue profiles between F2 and F3 with only less Gly taken up from the host cell. Notably, the ^{13}C-excess ratio of F2:F3 in Gly increased over time in the WT bacteria, but decreased in the Δ*zwf* mutant strain (SI Fig. 3), again indicating that the synthesis of Gly from glucose is *zwf*-dependent in *Lp*. Together, all these observations are in line with the conclusion that glucose is used throughout the intracellular growth.

3.5.3. Glucose is only a minor carbon source for the energy metabolism of intracellular Lp, but could serve a more prominent role in biosynthesis and as a growth regulator

The ^{13}C-experiments demonstrated for the first time that glucose from the host cell is utilized by intracellular *Lp* for its core metabolism *via* the ED pathway and TCA cycle. Hereby, glucose is metabolized already during the lag and early exponential phase of the bacterial growth cycle (Fig. 6). However, the absolute contributions of glucose as a source to drive the overall energy metabolism of *Lp* seemed to be small, when comparing the differences of ^{13}C-incorporation by *Lp* WT and the Δ*zwf* strain into PHB and amino acids derived from acetyl-CoA, pyruvate, and intermediates of the TCA cycle, respectively. In line with this, glucose also does not enhance bacterial growth or enhance oxygen consumption rates in broth cultivation, further contradicting its role as a main energy source (Weiss et al., 1980; Tesh and Miller, 1981; Tesh et al., 1983; Eylert et al. 2008; Häuslein et al., 2017). Nevertheless, exogenous glucose could serve as a more efficient precursor for anabolic processes such as providing the building units for peptidoglycan biosynthesis under intracellular conditions. Further studies are required to elucidate these upstream metabolic fluxes in a putatively bipartite metabolic network where amino acids serve as main substrates for energy generation and glucose or its phosphate as a source for cell wall and nucleic acid biosynthesis.

The importance of glucose especially for intracellular *Lp* is underlined by the finding that *Lp* strains with defects of the ED pathway were hampered for replication inside amoebae, but were not hindered when growing in broth (Eylert et al., 2010; Harada et al., 2010). The same behaviour holds true for mutants defective in inositol usage when comparing growth in amoebae with growth in broth (Manske et al., 2016).

Besides reduced rates of glucose utilization, the *Lp* Δ*zwf* strain used in this study also showed some differences in terms of Ser metabolization. This could add evidence for a regulatory role of intracellular glucose and related downstream metabolites in *Lp*, as already mentioned above. Interestingly, in *Francisella tularensis*, the "moonlight-protein" fructose-1,6-bisphosphate aldolase was shown to act as a global transcriptional regulator (Ziveri et al., 2017) and several enzymes of the ED pathway were shown to play multiple roles in Archaea (Lamble et al., 2003, 2004; Angelov et al., 2005). Indeed, the role of glucose as a nutrient and a signalling compound for intracellular *Lp* is underlined by the diverse environmental conditions for the bacterium. Before encountering a suitable host, *Lp* reside in fresh water as planktonic bacteria and biofilms without replicating (Steinert et al., 2002; Hilbi et al., 2011). Since fresh water only contains glucose in neglectable amounts in contrast to the cytosol of amoebae, glucose or carbohydrate levels could constitute a key signal for *Lp*, in addition to Cys and Thr (Sauer et al., 2005; Ewann and Hoffman, 2006), to identify the new intracellular environment suitable for replication. This role of glucose for intracellularly replicating *Lp* still needs to be further investigated as well as potential metabolic processes during the lag phase in general, which are only rudimentarily understood (Bertrand, 2019).

Declaration of Competing Interest

None.

Acknowledgments

This work was supported by the Deutsche Forschungsgemeinschaft (EI 384/11; HE 2845/9) and the Robert Koch Institute. WE and TS were also supported by the DFG through Project-ID 364653263 in the context of TRR 235.

Appendix A. Supplementary data

Supplementary material related to this article can be found, in the online version, at doi:https://doi.org/10.1016/j.ijmm.2021.151504.

References

Angelov, A., Futterer, O., Valerius, O., Braus, G.H., Liebl, W., 2005. Properties of the recombinant glucose/galactose dehydrogenase from the extreme thermoacidophile, *Picrophilus torridus*. FEBS J. 272 (4), 1054–1062. https://doi.org/10.1111/j.1742-4658.2004.04539.x.

Aurass, P., Pless, B., Rydzewski, K., Holland, G., Bannert, N., Flieger, A., 2009. bdhA-patD operon as a virulence determinant, revealed by a novel large-scale approach for identification of *Legionella pneumophila* mutants defective for amoeba infection. Appl. Environ. Microbiol. 75 (13), 4506–4515. https://doi.org/10.1128/AEM.00187-09.

Belyi, Y., Tabakova, I., Stahl, M., Aktories, K., 2008. Lgt: a family of cytotoxic glucosyltransferases produced by *Legionella pneumophila*. J. Bacteriol. 190 (8), 3026–3035. https://doi.org/10.1128/JB.01798-07.

Bertrand, R.L., 2019. Lag phase is a dynamic, organized, adaptive, and evolvable period that prepares bacteria for cell division. J. Bacteriol. 201 (7) https://doi.org/10.1128/JB.00697-18.

Best, A., Abu Kwaik, Y., 2019. Nutrition and bipartite metabolism of intracellular pathogens. Trends Microbiol. 27 (6), 550–561. https://doi.org/10.1016/j.tim.2018.12.012.

Best, A., Jones, S., Abu Kwaik, Y., 2018a. Mammalian solute carrier (SLC)-like transporters of *Legionella pneumophila*. Sci. Rep. 8 (1), 8352. https://doi.org/10.1038/s41598-018-26782-x.

Best, A., Price, C., Ozanic, M., Santic, M., Jones, S., Abu Kwaik, Y., 2018b. A *Legionella pneumophila* amylase is essential for intracellular replication in human macrophages and amoebae. Sci. Rep. 8 (1), 6340. https://doi.org/10.1038/s41598-018-24724-1.

Brüggemann, H., Cazalet, C., Buchrieser, C., 2006. Adaptation of *Legionella pneumophila* to the host environment: role of protein secretion, effectors and eukaryotic-like proteins. Curr. Opin. Microbiol. 9 (1), 86–94. https://doi.org/10.1016/j.mib.2005.12.009.

Byrne, B., Swanson, M.S., 1998. Expression of *Legionella pneumophila* virulence traits in response to growth conditions. Infect. Immun. 66 (8), 3029–3034.

Cazalet, C., Rusniok, C., Brüggemann, H., Zidane, N., Magnier, A., Ma, L., Tichit, M., Jarraud, S., Bouchier, C., Vandenesch, F., Kunst, F., Etienne, J., Glaser, P., Buchrieser, C., 2004. Evidence in the *Legionella pneumophila* genome for exploitation of host cell functions and high genome plasticity. Nat. Genet. 36 (11), 1165–1173. https://doi.org/10.1038/ng1447.

Cho, K.H., Caparon, M.G., 2008. tRNA modification by GidA/MnmE is necessary for *Streptococcus pyogenes* virulence: a new strategy to make live attenuated strains. Infect. Immun. 76 (7), 3176–3186. https://doi.org/10.1128/IAI.01721-07.

Cunha, C.B., Cunha, B.A., 2017. Legionnaire's disease since philadelphia: lessons learned and continued progress. Infect. Dis. Clin. North Am. 31 (1), 1–5. https://doi.org/10.1016/j.idc.2016.10.001.

Cunha, B.A., Burillo, A., Bouza, E., 2016. Legionnaires' disease. Lancet 387 (10016), 376–385. https://doi.org/10.1016/S0140-6736(15)60078-2.

De Leon, J.A., Qiu, J., Nicolai, C.J., Counihan, J.L., Barry, K.C., Xu, L., Lawrence, R.E., Castellano, B.M., Zoncu, R., Nomura, D.K., Luo, Z.Q., Vance, R.E., 2017. Positive and negative regulation of the master metabolic regulator mTORC1 by two families of *Legionella pneumophila* effectors. Cell Rep. 21 (8), 2031–2038. https://doi.org/10.1016/j.celrep.2017.10.088.

Eisenreich, W., Heuner, K., 2016. The life stage-specific pathometabolism of *Legionella pneumophila*. FEBS Lett. 590 (21), 3868–3886. https://doi.org/10.1002/1873-3468.12326.

Eisenreich, W., Rudel, T., Heesemann, J., Goebel, W., 2017. To eat and to be eaten: mutual metabolic adaptations of immune vells and intracellular bacterial pathogens upon Infection. Front. Cell. Infect. Microbiol. 7, 316. https://doi.org/10.3389/fcimb.2017.00316.

Eisenreich, W., Rudel, T., Heesemann, J., Goebel, W., 2019. How viral and intracellular bacterial pathogens reprogram the metabolism of host cells to allow their intracellular replication. Front. Cell. Infect. Microbiol. 9 https://doi.org/10.3389/fcimb.2019.00042.

Ewann, F., Hoffman, P.S., 2006. Cysteine metabolism in *Legionella pneumophila*: characterization of an *L*-cystine-utilizing mutant. Appl. Environ. Microbiol. 72 (6), 3993–4000. https://doi.org/10.1128/AEM.00684-06.

Eylert, E., Schär, J., Mertins, S., Stoll, R., Bacher, A., Goebel, W., Eisenreich, W., 2008. Carbon metabolism of *Listeria monocytogenes* growing inside macrophages. Mol. Microbiol. 69 (4), 1008–1017. https://doi.org/10.1111/j.1365-2958.2008.06337.x.

Eylert, E., Herrmann, V., Jules, M., Gillmaier, N., Lautner, M., Buchrieser, C., Eisenreich, W., Heuner, K., 2010. Isotopologue profiling of *Legionella pneumophila*: role of serine and glucose as carbon substrates. J. Biol. Chem. 285 (29), 22232–22243. https://doi.org/10.1074/jbc.M110.128678.

Farbrother, P., Wagner, C., Na, J., Tunggal, B., Morio, T., Urushihara, H., Tanaka, Y., Schleicher, M., Steinert, M., Eichinger, L., 2006. *Dictyostelium* transcriptional host cell response upon infection with *Legionella*. Cell. Microbiol. 8 (3), 438–456. https://doi.org/10.1111/j.1462-5822.2005.00633.x.

Faucher, S.P., Mueller, C.A., Shuman, H.A., 2011. *Legionella pneumophila* transcriptome during intracellular multiplication in human macrophages. Front. Microbiol. 2, 60. https://doi.org/10.3389/fmicb.2011.00060.

Faulkner, G., Garduno, R.A., 2002. Ultrastructural analysis of differentiation in *Legionella pneumophila*. J. Bacteriol. 184 (24), 7025–7041. https://doi.org/10.1128/jb.184.24.7025-7041.2002.

Fraser, D.W., Tsai, T.R., Orenstein, W., Parkin, W.E., Beecham, H.J., Sharrar, R.G., Harris, J., Mallison, G.F., Martin, S.M., McDade, J.E., Shepard, C.C., Brachman, P.S., 1977. Legionnaires' disease: description of an epidemic of pneumonia. N. Engl. J. Med. 297 (22), 1189–1197. https://doi.org/10.1056/NEJM197712012972201.

Garduno, R.A., Garduno, E., Hiltz, M., Hoffman, P.S., 2002. Intracellular growth of *Legionella pneumophila* gives rise to a differentiated form dissimilar to stationary-phase forms. Infect. Immun. 70 (11), 6273–6283. https://doi.org/10.1128/iai.70.11.6273-6283.2002.

Gillmaier, N., Götz, A., Schulz, A., Eisenreich, W., Goebel, W., 2012. Metabolic responses of primary and transformed cells to intracellular *Listeria monocytogenes*. PLoS One 7 (12), e52378. https://doi.org/10.1371/journal.pone.0052378.

Gillmaier, N., Schunder, E., Kutzner, E., Tlapak, H., Rydzewski, K., Herrmann, V., Stämmler, M., Lasch, P., Eisenreich, W., Heuner, K., 2016. Growth-related metabolism of the carbon storage poly-3-hydroxybutyrate in *Legionella pneumophila*. J. Biol. Chem. 291 (12), 6471–6482. https://doi.org/10.1074/jbc.M115.693481.

Grubmüller, S., Schauer, K., Goebel, W., Fuchs, T.M., Eisenreich, W., 2014. Analysis of carbon substrates used by *Listeria monocytogenes* during growth in J774A.1 macrophages suggests a bipartite intracellular metabolism. Front. Cell. Infect. Microbiol. 4, 156. https://doi.org/10.3389/fcimb.2014.00156.

Gupta, R., Gobble, T.R., Schuster, M., 2009. GidA posttranscriptionally regulates rhl quorum sensing in *Pseudomonas aeruginosa*. J. Bacteriol. 191 (18), 5785–5792. https://doi.org/10.1128/JB.00335-09.

Hammer, B.K., Swanson, M.S., 1999. Co-ordination of *Legionella pneumophila* virulence with entry into stationary phase by ppGpp. Mol. Microbiol. 33 (4), 721–731. https://doi.org/10.1046/j.1365-2958.1999.01519.x.

Harada, E., Iida, K., Shiota, S., Nakayama, H., Yoshida, S., 2010. Glucose metabolism in *Legionella pneumophila*: dependence on the Entner-Doudoroff pathway and connection with intracellular bacterial growth. J. Bacteriol. 192 (11), 2892–2899. https://doi.org/10.1128/JB.01535-09.

Häuslein, I., Manske, C., Goebel, W., Eisenreich, W., Hilbi, H., 2016. Pathway analysis using ^{13}C-glycerol and other carbon tracers reveals a bipartite metabolism of *Legionella pneumophila*. Mol. Microbiol. 100 (2), 229–246. https://doi.org/10.1111/mmi.13313.

Häuslein, I., Sahr, T., Escoll, P., Klausner, N., Eisenreich, W., Buchrieser, C., 2017. *Legionella pneumophila* CsrA regulates a metabolic switch from amino acid to glycerolipid metabolism. Open Biol. 7 (11) https://doi.org/10.1098/rsob.170149.

Herrmann, V., Eidner, A., Rydzewski, K., Bladel, I., Jules, M., Buchrieser, C., Eisenreich, W., Heuner, K., 2011. GamA is a eukaryotic-like glucoamylase responsible for glycogen- and starch-degrading activity of *Legionella pneumophila*. Int. J. Med. Microbiol. 301 (2), 133–139. https://doi.org/10.1016/j.ijmm.2010.08.016.

Heuner, K., Eisenreich, W., 2016. In: Unden, G., Thines, E., Schüffler, A. (Eds.), Crosstalk between Metabolism and Virulence of *Legionella pneumophila*. Host - Pathogen Interaction; Microbial Metabolism, Pathogenicity and Antiinfectives. Wiley-VCH Verlag GmbH & Co. KGaA, Weinheim, Germany, pp. 19–36.

Heuner, K., Brand, B.C., Hacker, J., 1999. The expression of the flagellum of *Legionella pneumophila* is modulated by different environmental factors. FEMS Microbiol. Lett. 175 (1), 69–77.

Heuner, K., Dietrich, C., Skriwan, C., Steinert, M., Hacker, J., 2002. Influence of the alternative sigma(28) factor on virulence and flagellum expression of *Legionella pneumophila*. Infect. Immun. 70 (3), 1604–1608.

Heuner, K., Kunze, M., Chen, F., Eisenreich, W., 2019. The pathometabolism of *Legionella* studied by isotopologue profiling. Methods Mol. Biol. 1921, 21–44. https://doi.org/10.1007/978-1-4939-9048-1_2.

Hilbi, H., Hoffmann, C., Harrison, C.F., 2011. *Legionella spp*. outdoors: colonization, communication and persistence. Environ. Microbiol. Rep. 3 (3), 286–296. https://doi.org/10.1111/j.1758-2229.2011.00247.x.

James, B.W., Mauchline, W.S., Dennis, P.J., Keevil, C.W., Wait, R., 1999. Poly-3-hydroxybutyrate in *Legionella pneumophila*, an energy source for survival in low-nutrient environments. Appl. Environ. Microbiol. 65 (2), 822–827.

Krawczyk, C.M., Holowka, T., Sun, J., Blagih, J., Amiel, E., DeBerardinis, R.J., Cross, J. R., Jung, E., Thompson, C.B., Jones, R.G., Pearce, E.J., 2010. Toll-like receptor-induced changes in glycolytic metabolism regulate dendritic cell activation. Blood 115 (23), 4742–4749. https://doi.org/10.1182/blood-2009-10-249540.

Laemmli, U.K., 1970. Cleavage of structural proteins during the assembly of the head of bacteriophage T4. Nature 227 (5259), 680–685.

Lamble, H.J., Heyer, N.I., Bull, S.D., Hough, D.W., Danson, M.J., 2003. Metabolic pathway promiscuity in the archaeon *Sulfolobus solfataricus* revealed by studies on glucose dehydrogenase and 2-keto-3-deoxygluconate aldolase. J. Biol. Chem. 278 (36), 34066–34072. https://doi.org/10.1074/jbc.M305818200.

Lamble, H.J., Milburn, C.C., Taylor, G.L., Hough, D.W., Danson, M.J., 2004. Gluconate dehydratase from the promiscuous Entner-Doudoroff pathway in *Sulfolobus solfataricus*. FEBS Lett. 576 (1–2), 133–136. https://doi.org/10.1016/j.febslet.2004.08.074.

Lau, R., Maqsood, S., Harte, D., Caughley, B., Deacon, R., 2013. Prevalence of *Legionella* strains in cooling towers and legionellosis cases in New Zealand. J. Environ. Health 75 (6), 82–89.

Lee, W.N., Byerley, L.O., Bergner, E.A., Edmond, J., 1991. Mass isotopomer analysis: theoretical and practical considerations. Biol. Mass Spectrom. 20 (8), 451–458. https://doi.org/10.1002/bms.1200200804.

Levanova, N., Mattheis, C., Carson, D., To, K.N., Jank, T., Frankel, G., Aktories, K., Schroeder, G.N., 2019. The *Legionella* effector LtpM is a new type of phosphoinositide-activated glucosyltransferase. J. Biol. Chem. 294 (8), 2862–2879. https://doi.org/10.1074/jbc.RA118.005952.

Lomma, M., Dervins-Ravault, D., Rolando, M., Nora, T., Newton, H.J., Sansom, F.M., Sahr, T., Gomez-Valero, L., Jules, M., Hartland, E.L., Buchrieser, C., 2010. The *Legionella pneumophila* F-box protein Lpp2082 (AnkB) modulates ubiquitination of the host protein parvin B and promotes intracellular replication. Cell. Microbiol. 12 (9), 1272–1291. https://doi.org/10.1111/j.1462-5822.2010.01467.x.

Manske, C., Schell, U., Hilbi, H., 2016. Metabolism of myo-inositol by *Legionella pneumophila* promotes infection of amoeba and macrophages. Appl. Environ. Microbiol. 82 (15), 5000–5014. https://doi.org/10.1128/AEM.01018-16.

Mehlitz, A., Eylert, E., Huber, C., Lindner, B., Vollmuth, N., Karunakaran, K., Goebel, W., Eisenreich, W., Rudel, T., 2017. Metabolic adaptation of *Chlamydia trachomatis* to mammalian host cells. Mol. Microbiol. 103 (6), 1004–1019. https://doi.org/10.1111/mmi.13603.

Mondino, S., Schmidt, S., Rolando, M., Escoll, P., Gomez-Valero, L., Buchrieser, C., 2020. Legionnaires' disease: state of the art knowledge of pathogenesis mechanisms of *Legionella*. Annu. Rev. Pathol. 15, 439–466. https://doi.org/10.1146/annurev-pathmechdis-012419-032742.

Oliva, G., Sahr, T., Buchrieser, C., 2018. The life cycle of *L. pneumophila*: cellular differentiation is linked to virulence and metabolism. Front. Cell. Infect. Microbiol. 8 (3) https://doi.org/10.3389/fcimb.2018.00003.

Price, C.T., Al-Khodor, S., Al-Quadan, T., Santic, M., Habyarimana, F., Kalia, A., Kwaik, Y.A., 2009. Molecular mimicry by an F-box effector of *Legionella pneumophila* hijacks a conserved polyubiquitination machinery within macrophages and protozoa. PLoS Pathog. 5 (12), e1000704 https://doi.org/10.1371/journal.ppat.1000704.

Price, C.T., Al-Quadan, T., Santic, M., Rosenshine, I., Abu Kwaik, Y., 2011. Host proteasomal degradation generates amino acids essential for intracellular bacterial growth. Science 334 (6062), 1553–1557. https://doi.org/10.1126/science.1212868.

Price, C.T., Richards, A.M., Abu Kwaik, Y., 2014. Nutrient generation and retrieval from the host cell cytosol by intra-vacuolar *Legionella pneumophila*. Front. Cell. Infect. Microbiol. 4, 111. https://doi.org/10.3389/fcimb.2014.00111.

Price, C., Jones, S., Mihelcic, M., Santic, M., Abu Kwaik, Y., 2020. Paradoxical pro-inflammatory responses by human macrophages to an *Amoebae* host-adapted *Legionella* effector. Cell Host Microbe 27 (4), 571–584. https://doi.org/10.1016/j.chom.2020.03.003 e577.

Rehl, J.M., Shippy, D.C., Eakley, N.M., Brevik, M.D., Sand, J.M., Cook, M.E., Fadl, A.A., 2013. GidA expression in *Salmonella* is modulated under certain environmental conditions. Curr. Microbiol. 67 (3), 279–285. https://doi.org/10.1007/s00284-013-0361-2.

Richardson, A.R., 2019. Virulence and metabolism. Microbiol. Spectr. 7 (2) https://doi.org/10.1128/microbiolspec.GPP3-0011-2018.

Robertson, P., Abdelhady, H., Garduno, R.A., 2014. The many forms of a pleomorphic bacterial pathogen-the developmental network of *Legionella pneumophila*. Front. Microbiol. 5, 670. https://doi.org/10.3389/fmicb.2014.00670.

Rowbotham, T.J., 1980. Preliminary report on the pathogenicity of *Legionella pneumophila* for freshwater and soil amoebae. J. Clin. Pathol. 33 (12), 1179–1183.

Rowbotham, T.J., 1986. Current views on the relationships between amoebae, *legionellae* and man. Isr. J. Med. Sci. 22 (9), 678–689.

Russell, D.G., Huang, L., VanderVen, B.C., 2019. Immunometabolism at the interface between macrophages and pathogens. Nat. Rev. Immunol. 19 (5), 291–304. https://doi.org/10.1038/s41577-019-0124-9.

Sauer, J.D., Bachman, M.A., Swanson, M.S., 2005. The phagosomal transporter A couples threonine acquisition to differentiation and replication of *Legionella pneumophila* in macrophages. Proc. Natl. Acad. Sci. U. S. A. 102 (28), 9924–9929. https://doi.org/10.1073/pnas.0502767102.

Schunder, E., Gillmaier, N., Kutzner, E., Herrmann, V., Lautner, M., Heuner, K., Eisenreich, W., 2014. Amino acid uptake and metabolism of *Legionella pneumophila* hosted by *Acanthamoeba castellanii*. J. Biol. Chem. 289 (30), 21040–21054. https://doi.org/10.1074/jbc.M114.570085.

Sha, J., Kozlova, E.V., Fadl, A.A., Olano, J.P., Houston, C.W., Peterson, J.W., Chopra, A. K., 2004. Molecular characterization of a glucose-inhibited division gene, gidA, that regulates cytotoxic enterotoxin of *Aeromonas hydrophila*. Infect. Immun. 72 (2), 1084–1095. https://doi.org/10.1128/iai.72.2.1084-1095.2004.

Steiner, B., Weber, S., Hilbi, H., 2018. Formation of the *Legionella*-containing vacuole: phosphoinositide conversion, GTPase modulation and ER dynamics. Int. J. Med. Microbiol. 308 (1), 49–57. https://doi.org/10.1016/j.ijmm.2017.08.004.

Steinert, M., Hentschel, U., Hacker, J., 2002. *Legionella pneumophila*: an aquatic microbe goes astray. FEMS Microbiol. Rev. 26 (2), 149–162. https://doi.org/10.1111/j.1574-6976.2002.tb00607.x.

Swart, A.L., Harrison, C.F., Eichinger, L., Steinert, M., Hilbi, H., 2018. *Acanthamoeba* and *Dictyostelium* as cellular models for *Legionella* infection. Front. Cell. Infect. Microbiol. 8, 61. https://doi.org/10.3389/fcimb.2018.00061.

Taylor, M., Ross, K., Bentham, R., 2009. *Legionella*, protozoa, and biofilms: interactions within complex microbial systems. Microb. Ecol. 58 (3), 538–547. https://doi.org/10.1007/s00248-009-9514-z.

Tesh, M.J., Miller, R.D., 1981. Amino acid requirements for *Legionella pneumophila* growth. J. Clin. Microbiol. 13 (5), 865–869. https://doi.org/10.1128/JCM.13.5.865-869.1981.

Tesh, M.J., Morse, S.A., Miller, R.D., 1983. Intermediary metabolism in *Legionella pneumophila*: utilization of amino acids and other compounds as energy sources. J. Bacteriol. 154 (3), 1104–1109.

Towbin, H., Staehelin, T., Gordon, J., 1979. Electrophoretic transfer of proteins from polyacrylamide gels to nitrocellulose sheets: procedure and some applications. Proc. Natl. Acad. Sci. U. S. A. 76 (9), 4350–4354.

Weiss, E., Peacock, M.G., Williams, J.C., 1980. Glucose and glutamate metabolism of *Legionella pneumophila*. Curr. Microbiol. 4 (1), 1–6. https://doi.org/10.1007/bf02602882.

Wieland, H., Ullrich, S., Lang, F., Neumeister, B., 2005. Intracellular multiplication of *Legionella pneumophila* depends on host cell amino acid transporter SLC1A5. Mol. Microbiol. 55 (5), 1528–1537. https://doi.org/10.1111/j.1365-2958.2005.04490.x.

Ziveri, J., Tros, F., Guerrera, I.C., Chhuon, C., Audry, M., Dupuis, M., Barel, M., Korniotis, S., Fillatreau, S., Gales, L., Cahoreau, E., Charbit, A., 2017. The metabolic enzyme fructose-1,6-bisphosphate aldolase acts as a transcriptional regulator in pathogenic *Francisella*. Nat. Commun. 8 (1), 853. https://doi.org/10.1038/s41467-017-00889-7.